International Astronomy and Astrophysics Research Journal

Volume 8, Issue 1, Page 94-101, 2026; Article no.IAARJ.164758

Recurrent X-Class Flare Activity from NOAA Active Region 4366 and Its Weak Geoeffective Response: A Case Study of the Solar-Terrestrial Event (1–6 February 2026)

Ashish Kumar Meena [a++*]

[a] *Department of Physics, SR University, Warangal, Telangana, India.*

Author's contribution

The sole author designed, analysed, interpreted and prepared the manuscript.

Article Information

DOI: https://doi.org/10.9734/iaarj/2026/v8i1127

Open Peer Review History:
This journal follows the Advanced Open Peer Review policy. Identity of the Reviewers, Editor(s) and additional Reviewers, peer review comments, different versions of the manuscript, comments of the editors, etc are available here: https://pr.sdiarticle5.com/review-history/164758

Original Research Article

Received: 23/06/2026
Accepted: 21/08/2026
Published: 24/08/2026

Abstract

Aims: To characterise the exceptionally dense sequence of X-class solar flares produced by NOAA Active Region 4366 and to examine why this energetic eruption sequence produced only a minor geomagnetic response at Earth.
Study Design: A bulletin-based observational case study synthesising publicly issued space-weather reports.
Place and Duration of Study: Data were compiled from bulletins issued by NOAA's Space Weather Prediction Center (SWPC), the Solar Influences Data Analysis Center (SIDC, Belgium), and NASA for the period 1–6 February 2026.
Methodology: Flare timing, magnitude, and active-region attribution were drawn from operational SWPC and SIDC bulletins and NASA Solar Dynamics Observatory imagery. Geomagnetic storm classification was

[++] *Post Doctor Fellow;*
**Corresponding author: E-mail: ashishmeena944@gmail.com;*

Cite as: *Meena, A. K. (2026). Recurrent X-Class Flare Activity from NOAA Active Region 4366 and Its Weak Geoeffective Response: A Case Study of the Solar-Terrestrial Event (1–6 February 2026). International Astronomy and Astrophysics Research Journal, 8(1), 94–101. https://doi.org/10.9734/iaarj/2026/v8i1127*

based on the SIDC's real-time planetary Kp index and the Belgian local K-index (K_BEL). A reproducible data-source table and an X-class event chronology table are provided. Causal language has been aligned with the bulletin-based nature of the dataset.
Results: AR 4366 produced six X-class flares, including an X8.1 event at 23:57 UT on 1 February 2026, which was among the strongest of Solar Cycle 25, together with 21 C-class and 38 M-class flares between 1 and 5 February 2026. Despite this activity, the associated magnetic cloud produced only a minor geomagnetic storm (planetary Kp = 5) on 4–5 February 2026, with no visible aurora reported from Belgium under the cited SIDC conditions.
Conclusion: The observed mismatch between eruptive intensity and geoeffectiveness is consistent with the established understanding that CME propagation geometry and solar-wind/IMF coupling strongly influence the geomagnetic response rather than flare X-ray class alone. This finding underscores the continued need for coronagraphic CME tracking and upstream L1 solar-wind monitoring in operational space-weather forecasting.

Keywords: Solar flares; Active Region 4366; coronal mass ejection; geomagnetic storm; Kp index; space weather forecasting.

1. Introduction

Solar flares and their associated coronal mass ejections (CMEs) constitute the principal drivers of geomagnetic disturbance at Earth, and periods of concentrated high-class flare activity from a single active region provide valuable natural experiments for solar-terrestrial coupling research (Gonzalez *et al*., 1994; Gopalswamy *et al*., 2001). Related case-based analyses have similarly examined coronal mass ejection and solar flare characteristics (Meena *et al*., 2022) and geomagnetic storms occurring in association with solar activity (Vaswani *et al*., 2022). In late January 2026, NOAA Active Region 4366 emerged and rapidly developed into a magnetically complex beta-gamma-delta sunspot group, becoming the dominant source of solar eruptive activity on the Earth-facing solar disk through the first week of February 2026.

Recent studies using physics-based forecasting and contemporary event analyses further support the evaluation of CME geoeffectiveness through propagation, interplanetary magnetic-field conditions, and compound ICME structure rather than flare class alone (Maharana *et al*., 2024; Hayakawa *et al*., 2025). Complementary studies of CME propagation and Solar Cycle 25 storm drivers likewise emphasise that heliospheric evolution and interplanetary driver structure are central to interpreting geomagnetic outcomes (Tyagi & Mishra, 2026; Onyemaechi *et al*., 2026).

This paper compiles and synthesises the publicly issued space-weather bulletins describing AR 4366's flare output and its geomagnetic consequence, with the specific aim of examining why an exceptionally energetic flare sequence, including an X8.1 event that was one of the strongest flares of Solar Cycle 25 to date, produced only a minor geomagnetic response at Earth. This deliberately narrow, well-documented case is used to illustrate the physical decoupling that can occur between solar flare class and geomagnetic storm intensity, a decoupling with direct relevance to operational space-weather forecasting. Although the manuscript establishes the general physical decoupling between flare class and geomagnetic response, the evidence assembled here leaves an event-specific research gap: a consolidated account is needed to relate AR 4366's dense X-class flare sequence to its reported minor geomagnetic response while preserving the limitations of bulletin-based observations. The present case study addresses this gap without assigning quantitative contributions to solar-wind or IMF parameters that were not included in the dataset.

Accordingly, the objective of this study is to synthesise the reported 1–6 February 2026 activity of NOAA AR 4366 and examine, within the limits of the available operational bulletins, the observed mismatch between the region's intense X-class flare activity and the reported minor geomagnetic response at Earth.

2. Methodology

This study is deliberately scoped as an event-report synthesis rather than a full statistical time-series analysis. Because a continuous, quality-controlled archived instrumental record (finalised GFZ Potsdam Kp/ap series, definitive WDC Kyoto Dst series, and high-resolution L1 solar-wind plasma/IMF data from DSCOVR or ACE) was not incorporated into the present manuscript at the time of preparation, the analysis relies on operational bulletins. Future work should incorporate these finalised datasets once fully quality-controlled versions become available.

Flare timing, magnitude, and active-region attribution were drawn from NOAA's Space Weather Prediction Center (SWPC) operational bulletins published through spaceweather.gov, the SIDC (Royal Observatory of Belgium) solar bulletin, and NASA Solar Dynamics Observatory imagery releases (NASA Solar Dynamics Observatory, 2026; NOAA Space Weather Prediction Center, 2026; Solar Influences Data Analysis Center [SIDC/STCE], 2026). Geomagnetic storm classification was taken from the SIDC's real-time reporting of the planetary Kp index and the Belgian local K-index (K_BEL). All flare times are reported in Universal Time (UT), and flare magnitudes follow the standard GOES 1–8 Å classification (A, B, C, M, X), in which each letter class denotes a tenfold increase in peak X-ray flux over the preceding class. Because this study relies on operational bulletins rather than a finalised post-event archive, cumulative flare-class tallies should be read as bulletin-time snapshots rather than a final definitive count.

Table 1. Data sources used in this study (reproducibility table)

Variable	Source / Agency	Product / Bulletin	Time Res.	Access Date	Status
X-ray flares	NOAA/SWPC	GOES XRS event lists; SWPC Daily Discussion & PRF	Event-based	Feb 2026	Real-time / Preliminary
Active-region attribution	NOAA/SWPC; NASA/SDO	SWPC Region Summaries; SDO/HMI magnetograms	Daily	Feb 2026	Operational
CME trajectory / geometry	NOAA/SWPC; SOHO/LASCO	SWPC Forecast Discussion; LASCO C2/C3 imagery	Event-based	Feb 2026	Modelled / Preliminary
Planetary Kp	SIDC / GFZ	SIDC real-time Kp; preliminary Kp	3-hourly	Feb 2026	Real-time / Preliminary
Local K-index (Belgium)	SIDC / STCE	K_BEL	3-hourly	Feb 2026	Real-time
SDO imagery	NASA/SDO	AIA / HMI continuum & magnetograms	Image cadence	Feb 2026	Public release

Note: Exact bulletin product names, permanent URLs, and access dates should be verified and expanded in the final version. No L1 solar-wind or definitive Dst data were incorporated; this is an explicit limitation (see Section 3.4)

3. Results and Discussion

3.1 Chronology of X-class Flare Activity

Six X-class flares were recorded from AR 4366 between 1 and 4 February 2026 (Fig. 1 and Table 2): an X1.0 flare at 12:33 UT and an X8.1 flare at 23:57 UT on 1 February; an X2.8 flare at 00:36 UT and an X1.6 flare at 08:14 UT on 2 February; an X1.5 flare on 3 February; and an X4.2 flare at 12:13 UT on 4 February. The X8.1 event was the largest of the sequence and one of the strongest flares of Solar Cycle 25 to date, associated with rapid magnetic expansion of the active region into a beta-gamma-delta configuration exceeding 500 microhemispheres in area.

3.2 Flare-class Distribution

As of the 5 February 2026 SWPC bulletin, AR 4366 had produced 21 C-class and 38 M-class flares since its emergence on 30 January, alongside the six X-class events described above (Fig. 2). This distribution illustrates a high level of productivity of mid- and high-energy events relative to the lower C-class category, a signature consistent with a magnetically complex, highly sheared active-region configuration (Schrijver, 2007; Toriumi & Wang, 2019). No formal statistical comparison with a baseline population of similarly complex regions is presented; the description remains qualitative and bulletin-time based.

Table 2. Chronology of X-class flares from NOAA AR 4366 (1–4 February 2026)

Date (UT)	Peak Time	GOES Class	NOAA AR	Location (approx.)	Notes / CME association
1 Feb 2026	12:33	X1.0	4366	N14E40	Part of intense sequence
1 Feb 2026	23:57	X8.1	4366	~N14	Strongest of sequence; CME modelled as glancing
2 Feb 2026	00:36	X2.8	4366	N14E30	Type II radio sweep reported
2 Feb 2026	08:14	X1.6	4366	N14E30	Optical 2B reported
3 Feb 2026	14:08	X1.5	4366	N14E14	No clear CME signature reported
4 Feb 2026	12:13	X4.2	4366	Near central	No clear CME signature at press time

Sources: NOAA/SWPC Daily Discussion and Preliminary Reports of Solar Geophysical Activity (PRF); NASA/SDO imagery releases. Times are peak times in UT. Locations are approximate from SWPC region reports

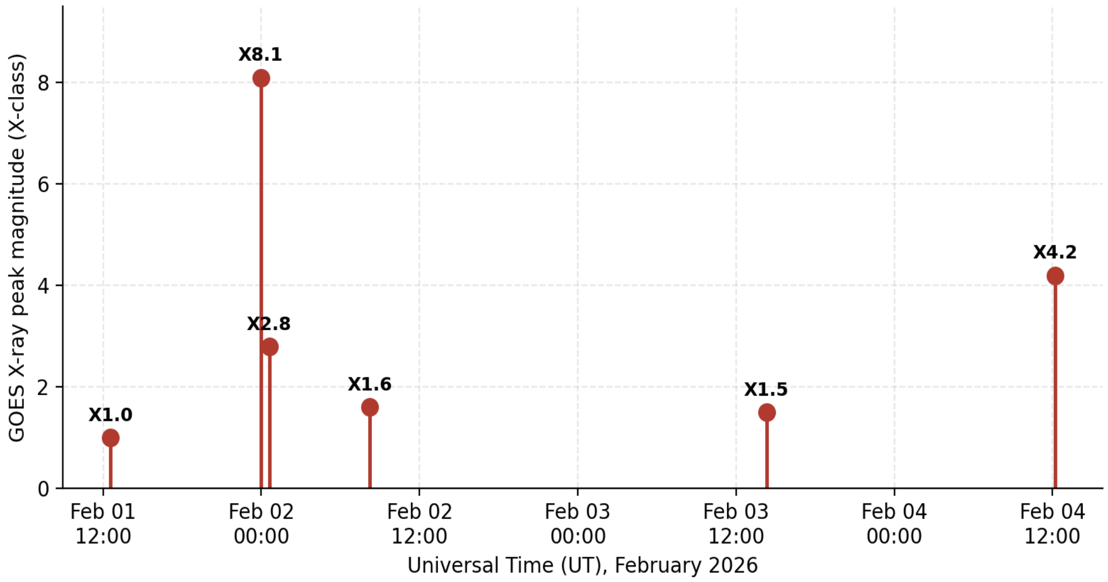

Fig. 1. Temporal sequence of the six X-class flares produced by NOAA AR 4366 between 1 and 4 February 2026, plotted by GOES peak magnitude. Source data: NOAA/SWPC GOES XRS event lists and Daily Discussion bulletins (operational, real-time products); figure is author-constructed from tabulated peak magnitudes and times

3.3 CME Transit and Geomagnetic Response

Despite the severity of the X8.1 flare, initial coronagraphic modelling indicated that the bulk of the associated CME material would pass Earth to the north and east, suggesting a glancing rather than direct impact. The associated magnetic cloud arrived at Earth's magnetosphere on 4 February 2026. According to SIDC reporting, the cloud only brushed the magnetosphere as expected, producing a minor geomagnetic storm with a planetary Kp index of 5, confirmed independently by the Belgian local K-index (K_BEL = 5). This was too weak to produce visible aurora at Belgian latitude under the cited SIDC conditions; the disturbance was reported as still ongoing but not expected to intensify substantially (Fig. 3). No systematic survey of high-latitude European or global auroral reports was performed; the statement is therefore restricted to the geographic scope supported by the operational evidence.

The central observational finding of this case study is the marked mismatch between flare energetics and geomagnetic consequence. An X8.1 flare represents one of the most energetic eruptions of the current solar cycle, yet its terrestrial geomagnetic signature was classified only as minor (Kp = 5). Several physical factors, drawn from established solar-terrestrial physics, plausibly account for this: (i) the modelled CME trajectory placed the bulk of ejected material to the north and east of the Sun–Earth line, indicating a glancing rather than head-on encounter; (ii) SIDC radio observations found no clear signature of a magnetic cloud accompanying at least one of the X-class eruptions, suggesting that not every X-class flare in the sequence was CME-productive; and (iii) the active region's location and evolving magnetic connectivity through the observation window affected which eruptions were geoeffectively directed at Earth.

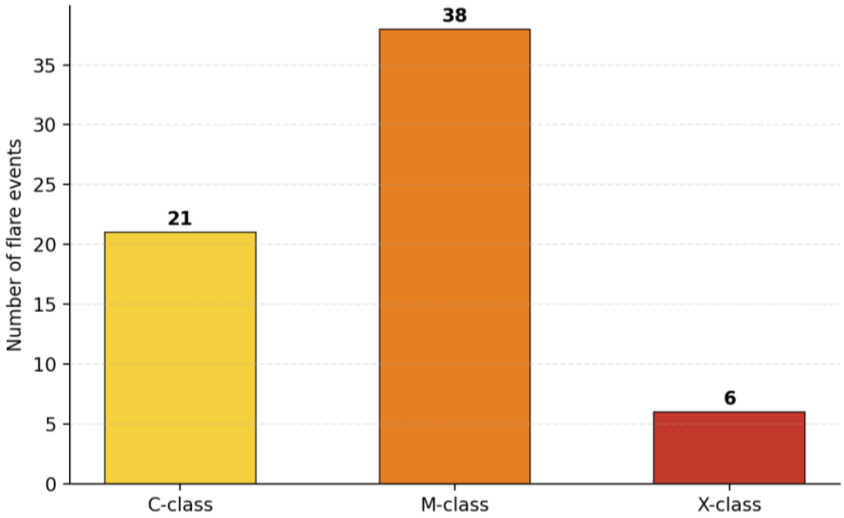

Fig. 2. Cumulative GOES flare-class tally attributed to AR 4366, as reported by NOAA/SWPC on 5 February 2026 (bulletin-time snapshot; not a finalized post-event count). Source: NOAA/SWPC region summary / Daily Discussion of 5 February 2026; figure is author-constructed from the reported cumulative counts

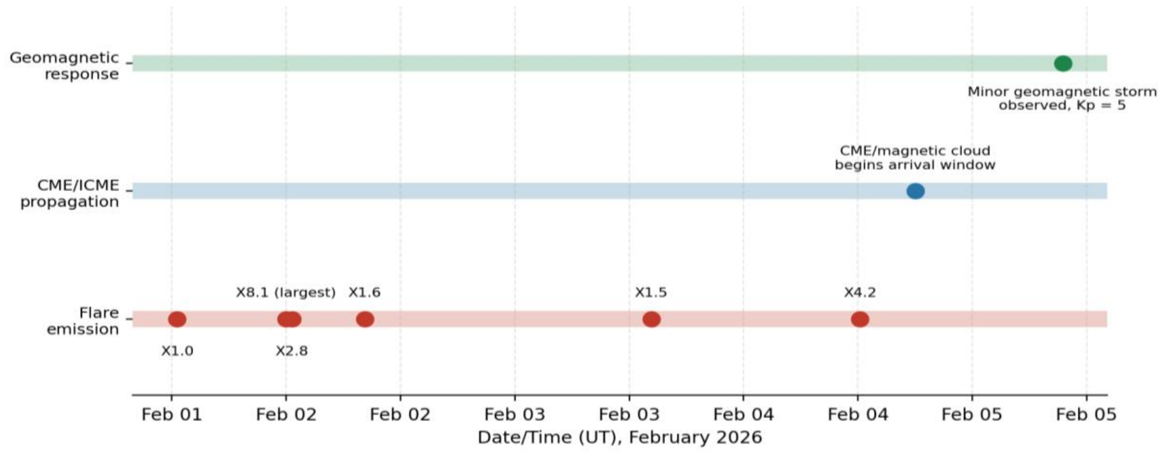

Fig. 3. Schematic event chain linking the X-class flare sequence, CME/magnetic-cloud transit, and the observed minor (Kp = 5) geomagnetic response. This is a qualitative event-timing diagram, not a continuous index time series, reflecting the bulletin-based nature of the source data. Source: NOAA/SWPC, SIDC

Source: Author-constructed schematic based on NOAA/SWPC Forecast Discussions and SIDC real-time Kp / K_BEL reports; not derived from a continuous instrumental time series

It is important to emphasise that storm magnitude is controlled by a combination of factors, including ICME/sheath field magnitude, southward Bz magnitude and duration, solar-wind speed, density/dynamic pressure, magnetic structure, possible CME–CME interaction, and magnetopause coupling efficiency (Burton *et al*., 1975; O'Brien & McPherron, 2000; Gonzalez *et al*., 1994). The present bulletin-based dataset does not include upstream L1 solar-wind plasma or IMF measurements; therefore, the relative contribution of trajectory versus magnetic orientation cannot be quantitatively partitioned. The observed mismatch is consistent with the well-established principle that flare X-ray class alone is a poor predictor of geomagnetic storm intensity; the dominant controls lie with CME kinematics, magnetic-field orientation (particularly the southward Bz component), and solar-wind coupling efficiency at the magnetopause (Maharana *et al*., 2024).

The February 2026 AR 4366 sequence, considered against historically extreme analogues such as the October–November 2003 "Halloween storms" from AR 10486, which produced comparable or greater X-class flare output alongside severe geomagnetic storms reaching Dst minima below −350 nT (Gopalswamy *et al*., 2005), illustrates that flare magnitude and storm severity can diverge sharply depending on eruption geometry and interplanetary conditions. Complementary perspectives from ionospheric response studies (Meena & Gour, 2024; Meena, Gour, *et al*., 2024; Meena, Sharma, *et al*., 2024a, 2024b) and correlation analyses of solar activity indices with geomagnetic disturbance (Gour *et al*., 2024) provide additional context, although the core literature on CME/ICME geoeffectiveness remains the primary interpretive framework.

4. Limitations

This study is explicitly scoped as a bulletin-based case-study synthesis rather than a statistical analysis of archived instrumental time series. Specific limitations include: (i) flare-class tallies are drawn from an operational bulletin issued mid-sequence (5 February) and are not a finalised post-event count; (ii) no finalised Dst index value is reported here, as WDC Kyoto's definitive (as opposed to quicklook/real-time) Dst record for this interval was not incorporated; (iii) no upstream L1 solar-wind plasma or interplanetary magnetic field data (e.g., from DSCOVR or ACE) were incorporated, which would be required to quantitatively attribute the muted geomagnetic response to specific solar-wind driver parameters rather than to CME trajectory alone. Future work extending this case study should incorporate the finalised GFZ Potsdam Kp/ap series, the definitive WDC Kyoto Dst record, and L1 in situ solar-wind measurements once these become available in their post-event, quality-controlled form. Complementary perspectives from energy-resolved cosmic-ray particle-detector networks (Meena, 2026) and comparative planetary ionospheric studies (Harada *et al*., 2018) may further help contextualise the geoeffectiveness of dense X-class flare sequences such as this one.

5. Conclusion

NOAA Active Region 4366 produced six X-class flares between 1 and 4 February 2026, including an X8.1 event that was among the strongest flares of Solar Cycle 25, while bulletin-time reporting also documented substantial C- and M-class activity. Nevertheless, the magnetic-cloud arrival on 4–5 February produced only a minor geomagnetic storm, with planetary Kp = 5 and K_BEL = 5, and no visible aurora was reported from Belgium under the cited conditions. The case demonstrates a clear observational mismatch between flare intensity and the reported geomagnetic response. Within the limits of the bulletin-based dataset, the glancing CME geometry provides a plausible explanation for the weak terrestrial effect, but the relative influence of CME trajectory and magnetic-field orientation cannot be quantified because upstream L1 solar-wind plasma and IMF measurements were not incorporated. The event therefore reinforces the need to interpret flare class together with CME propagation geometry and solar-wind coupling. Finalised geomagnetic indices and in situ solar-wind observations would be required for a more complete post-event characterisation.

Consent

It is not applicable.

Ethical Approval

It is not applicable.

Declaration of AI Use

This manuscript was prepared through the intellectual contributions of the author(s) to the study design, data analysis, interpretation of results, and scholarly content. Grammarly and ChatGPT were used solely to assist with grammatical refinement and reference formatting during manuscript revision. The author(s) accept full responsibility for the accuracy, integrity, and final content of the manuscript.

Competing Interests

Author has declared that there is no known competing financial interests or non-financial interests or personal relationships that could have appeared to influence the work reported in this paper.

References

Burton, R. K., McPherron, R. L., & Russell, C. T. (1975). An empirical relationship between interplanetary conditions and Dst. *Journal of Geophysical Research, 80*(31), 4204–4214. https://doi.org/10.1029/JA080i031p04204

Gonzalez, W. D., Joselyn, J. A., Kamide, Y., Kroehl, H. W., Rostoker, G., Tsurutani, B. T., & Vasyliunas, V. M. (1994). What is a geomagnetic storm? *Journal of Geophysical Research: Space Physics, 99*(A4), 5771–5792. https://doi.org/10.1029/93JA02867

Gopalswamy, N., Lara, A., Yashiro, S., Kaiser, M. L., & Howard, R. A. (2001). Predicting the 1-AU arrival times of coronal mass ejections. *Journal of Geophysical Research: Space Physics, 106*(A12), 29207–29217. https://doi.org/10.1029/2001JA000177

Gopalswamy, N., Yashiro, S., Liu, Y., Michalek, G., Vourlidas, A., Kaiser, M. L., & Howard, R. A. (2005). Coronal mass ejections and other extreme characteristics of the 2003 October–November solar eruptions. *Journal of Geophysical Research: Space Physics, 110*(A9), Article A09S15. https://doi.org/10.1029/2004JA010958

Gour, P. S., Meena, A. K., Verma, P. L., Soni, S., Sharma, J., & Yadav, V. (2024). Correlation analysis of key parameters associated with solar activity and geomagnetic disturbances throughout 2023. *European Academic Research, 11*(12), 1494–1504. https://euacademic.org/UploadArticle/5943.pdf

Harada, Y., Gurnett, D. A., Kopf, A. J., Halekas, J. S., Ruhunusiri, S., DiBraccio, G. A., Espley, J., & Brain, D. A. (2018). MARSIS observations of the Martian nightside ionosphere during the September 2017 solar event. *Geophysical Research Letters, 45*(16), 7960–7967. https://doi.org/10.1002/2018GL077622

Hayakawa, H., Ebihara, Y., Mishev, A., Koldobskiy, S., Kusano, K., Bechet, S., Yashiro, S., Iwai, K., Shinbori, A., Mursula, K., Miyake, F., Shiota, D., Silveira, M. V. D., Stuart, R., Oliveira, D. M., Akiyama, S., Ohnishi, K., Ledvina, V., & Miyoshi, Y. (2025). The solar and geomagnetic storms in 2024 May: A flash data report. *The Astrophysical Journal, 979*(1), Article 49. https://doi.org/10.3847/1538-4357/ad9335

Maharana, A., Cramer, W. D., Samara, E., Scolini, C., Raeder, J., & Poedts, S. (2024). Employing the coupled EUHFORIA-OpenGGCM model to predict CME geoeffectiveness. *Space Weather, 22*(5), e2023SW003715. https://doi.org/10.1029/2023SW003715

Meena, A. K. (2026). Spectral discrimination of ground level enhancements and magnetospheric effects using energy-resolved muon and neutron measurements from the SEVAN light detector network. *British Journal of Contemporary Research, 1*(3), Article 008. https://doi.org/10.67693/bjcr-m77chxh8

Meena, A. K., & Gour, P. S. (2024). Investigating Asia's low-latitude ionosphere's pulse during the spectacular September 2017 solar storms. *Tuijin Jishu/Journal of Propulsion Technology, 45*(1), 3322–3334. https://www.propulsiontechjournal.com/index.php/journal/article/download/4780/3277/8273

Meena, A. K., Gour, P. S., & Soni, S. (2024). The effects of strong and weak solar flares on the total electron content in the ionospheric ionosphere during the 2011 solar peak. *African Journal of Biomedical Research, 27*(4S), 2422–2433. https://doi.org/10.53555/AJBR.v27i4S.2421

Meena, A. K., Sharma, A., & Gour, P. S. (2024a). Ionospheric responses to solar flares: An analysis of ion composition changes during moderately high solar activity in January 2023. *World Journal of Advanced Research and Reviews, 21*(3), 219–224. https://doi.org/10.30574/wjarr.2024.21.3.0618

Meena, A. K., Sharma, A., & Gour, P. S. (2024b). The impact of moderate solar flare activity on ionospheric response from August 5th to 7th, 2023. *World Journal of Advanced Research and Reviews, 22*(1), 43–54. https://doi.org/10.30574/wjarr.2024.22.1.1016

Meena, M. K., Meena, A. K., & Gour, P. S. (2022). Analysis of coronal mass ejections and solar flares. *International Journal of Innovative Research & Growth, 11*(3), 70–73. https://doi.org/10.26671/IJIRG.2022.3.11.104

NASA Solar Dynamics Observatory. (2026). *AIA and HMI imagery releases for Active Region 4366, February 1–5, 2026*. Retrieved February 2026, from https://sdo.gsfc.nasa.gov/

NOAA Space Weather Prediction Center. (2026). *Daily discussion and forecast products, preliminary reports of solar geophysical activity, and GOES XRS event lists for February 1–6, 2026*. Retrieved February 2026, from https://www.swpc.noaa.gov/

O'Brien, T. P., & McPherron, R. L. (2000). An empirical phase space analysis of ring current dynamics: Solar wind control of injection and decay. *Journal of Geophysical Research: Space Physics, 105*(A4), 7707–7719. https://doi.org/10.1029/1998JA000437

Onyemaechi, U. A., Onuchukwu, C. C., & Okoli, V. C. (2026). Solar-cycle modulation of narrow, normal, and wide coronal mass ejections: Comparative insights into kinematics, occurrence patterns, and propagation dynamics. *Asian Basic and Applied Research Journal, 8*(1), 400–427. https://doi.org/10.56557/abaarj/2026/v8i1234

Schrijver, C. J. (2007). A characteristic magnetic field pattern associated with all major solar flares and its use in flare forecasting. *The Astrophysical Journal, 655*(2), L117–L120. https://doi.org/10.1086/511857

Solar Influences Data Analysis Center (SIDC/STCE). (2026). *Real-time planetary Kp index and Belgian local K-index (K_BEL) reports for February 4–5, 2026*. Retrieved February 2026, from https://www.sidc.be/

Toriumi, S., & Wang, H. (2019). Flare-productive active regions. *Living Reviews in Solar Physics, 16*, Article 3. https://doi.org/10.1007/s41116-019-0019-7

Tyagi, P., & Mishra, V. K. (2026). Geoeffectiveness of interplanetary storm drivers during Solar Cycle 25 through June 2026: A comparative study of ICMEs, sheath regions, and corotating interaction regions. *Physical Science International Journal, 30*(5), 15–29. https://doi.org/10.9734/psij/2026/v30i5967

Vaswani, L. K., Gour, P. S., Meena, A. K., & Soni, S. (2022). Geomagnetic storm in association with solar activities. *International Journal of Innovative Research & Growth, 11*(4), 143–148. https://doi.org/10.26671/IJIRG.2022.4.11.103

Peer-review history:
The peer review history for this paper can be accessed here:
https://pr.sdiarticle5.com/review-history/164758